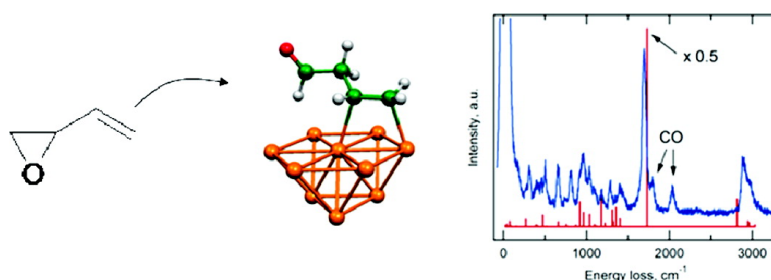Article

Adsorption and Reaction of 1-Epoxy-3-butene on Pt(111): Implications for Heterogeneous Catalysis of Unsaturated Oxygenates

Andrea S. Loh, Scott W. Davis, and J. Will Medlin

More About This Article

Additional resources and features associated with this article are available within the HTML version:

- Supporting Information
- Links to the 1 articles that cite this article, as of the time of this article download
- Access to high resolution figures
- Links to articles and content related to this article
- Copyright permission to reproduce figures and/or text from this article

View the Full Text HTML

Adsorption and Reaction of 1-Epoxy-3-butene on Pt(111): Implications for Heterogeneous Catalysis of Unsaturated Oxygenates

Andrea S. Loh, Scott W. Davis, and J. Will Medlin*

Department of Chemical and Biological Engineering, University of Colorado, Boulder, Colorado 80309-0424

Received December 14, 2007; E-mail: will.medlin@colorado.edu

Abstract: High-resolution electron energy loss spectroscopy (HREELS), temperature-programmed desorption (TPD), and density functional theory (DFT) calculations were used to study the adsorption and reaction of 1-epoxy-3-butene (EpB) on Pt(111). These investigations were conducted to help elucidate mechanisms for improving olefin hydrogenation selectivity in reactions of unsaturated oxygenates. EpB dosed to Pt(111) at 91 K adsorbs molecularly on the surface through the vinyl group with apparent rehybridization to a di-σ-bound state. By 233 K, however, EpB undergoes epoxide ring opening to form an aldehyde intermediate, which further decomposes upon heating to yield gas phase products CO, H_2, and propylene. Comparison of the HREELS and TPD data to experiments performed with 2-butenal (crotonaldehyde) shows that EpB and 2-butenal decompose through related pathways. However, the EpB-derived aldehyde intermediate clearly has a unique structure, features of which have been elucidated by DFT calculations. In conjunction with previous surface science studies of EpB chemistry, these results can help explain selectivity trends for reactions of EpB on Pt catalysts and bimetallic PtAg catalysts, with indications that the enhanced olefin hydrogenation selectivity of PtAg catalysts likely originates from a bifunctional effect.

1. Introduction

The design of solid catalysts for high selectivity is one of the major objectives of modern research in heterogeneous catalysis.[1] A particular challenge is the preparation of catalysts that enable high selectivity toward the conversion of a single functional group in a multifunctional molecule, thereby directing selectivity toward a particular product.[2] This need for high selectivity toward a single functional group may be of growing importance in efforts to establish biorefining operations, where biomass-derived multifunctional carbohydrates must be converted to commodity chemicals.[3]

One reaction of interest is the hydrogenation of 1-epoxy-3-butene (EpB). Not only is EpB hydrogenation important for industrial processes[4] but it also serves as a useful probe reaction for studying mechanisms for controlling the selectivity of reactions of multifunctional molecules containing both oxygenate and unsaturated functions. EpB is a simple four-carbon molecule containing both an olefin and an epoxide functionality. Reaction of EpB with hydrogen can proceed through two desired pathways: olefin hydrogenation to yield 1-epoxybutane and epoxide hydrogenolysis to produce unsaturated primary alcohols. Although both olefin hydrogenation and epoxide hydrogenolysis can lead to desired products, selectivity control is needed to reduce separation cost and to prevent hydrogenation of both functions, which yields less valuable products. Designing catalysts for the selective hydrogenation of the olefin function of EpB provides a special challenge associated with preventing ring-opening reactions in hydrogenation catalysis.

Previous investigations have focused on determining how the selectivity to certain products in EpB hydrogenation varies for different supported metal catalysts. Bartok et al. studied the hydrogenation and isomerization of EpB on Cu−SiO₂ catalysts.[5] In the absence of hydrogen, they found that the main product was *trans*-crotonaldehyde via isomerization. With hydrogen, 1,3-butadiene was the primary product formed through deoxygenation. 2,5-Dihydrofuran and *trans*- and *cis*-crotonaldehyde were also minor products formed. Bartok et al. also investigated EpB reactions over Pt/SiO₂ and Pd/SiO₂ catalysts.[6] With the Pt catalyst, they found that EpB underwent hydrogenation to yield epoxybutane as well as deoxygenation to form 1-butene and butane. On the Pd/SiO₂ catalyst, the dominant product under hydrogenation conditions was *trans*-crotonaldehyde, though epoxybutane was also formed as a secondary product.

(1) Somorjai, G. A.; Yang, M. C. *Top. Catal.* **2003**, *24*, 61–72.
(2) (a) Mohr, C.; Hofmeister, H.; Radnik, J.; Claus, P. *J. Am. Chem. Soc.* **2003**, *125*, 1905–1911. (b) Semagina, N.; Grasemann, M.; Xanthopoulos, N.; Renken, A.; Kiwi-Minsker, L. *J. Catal.* **2007**, *251*, 213–222. (c) Gebauer-Henke, E.; Grams, J.; Szubiakiewicz, E.; Farbotko, J.; Touroude, R.; Rynkowski, J. *J. Catal.* **2007**, *250*, 195–208. (d) Pei, Y.; Guo, P. J.; Qiao, M. H.; Li, H. X.; Wei, S. Q.; He, H. Y.; Fan, K. *J. Catal.* **2007**, *248*, 303–310.
(3) (a) Creamer, N. J.; Mikheenko, I. P.; Yong, P.; Deplanche, K.; Sanyahumbi, D.; Wood, J.; Pollmann, K.; Merroun, M.; Selenska-Pobell, S.; Macaskie, L. E. *Catal. Today* **2007**, *128*, 80–87. (b) Davda, R. R.; Shabaker, J. W.; Huber, G. W.; Cortright, R. D.; Dumesic, J. A. *Appl. Catal. B: Environ.* **2005**, *56*, 171–186.
(4) Armor, J. N. *Appl. Catal. A: Gen.* **2001**, *222*, 407–426.
(5) Bartok, M.; Fasi, A.; Notheisz, F. *J. Mol. Catal. A: Chem.* **1998**, *135*, 307–316.
(6) Bartok, M.; Fasi, A.; Notheisz, F. *J. Catal.* **1998**, *175*, 40–47.

One proposed method to improve selectivity is the use of bimetallic catalysts. Monnier and co-workers prepared a series of Ag–Pt/SiO$_2$ catalysts by depositing different weight loadings of Ag onto a Pt/SiO$_2$ catalyst using electroless deposition.[7] It was found that a loading of ¼ ML of Ag enhanced the selectivity to epoxybutane from 33 to 55% compared to the Ag-free catalyst while also increasing the overall EpB reaction rate. The same group also studied the hydrogenation of EpB over Cu–Pd/SiO$_2$, prepared by electroless deposition of Cu onto a Pd/SiO$_2$ catalyst.[8] As Cu coverage on the Pd/SiO$_2$ catalyst was increased from 0 to 0.37 ML, selectivity to unsaturated products (including 3-buten-1-ol, crotonaldehyde, and 2-buten-1-ol) increased from 50 to 75%. For both Ag–Pt and Cu–Pd catalysts, reasons for the trends in selectivity are not well-understood. An understanding of the performance of bimetallic catalysts first requires knowledge of the molecular-scale interactions between EpB and metal surfaces. More generally, surface studies of the interaction of multifunctional molecules on metals are needed to better understand selectivity trends and potentially enable the design of more selective catalysts.

One such study has been reported previously for EpB. Medlin et al. investigated the adsorption and reaction of EpB on Ag(110).[9,10] They found that EpB undergoes activated ring opening to form an oxametallacycle intermediate. Upon heating during temperature-programmed desorption (TPD) experiments, the intermediate undergoes 1,2- and 1,4-ring closure to form EpB and 2,5-dihydrofuran. Such oxametallacycle intermediates have also been observed after higher-temperature exposures of ethylene oxide and styrene oxide on Ag(110) and Ag(111).[11–13] Since the EpB-derived oxametallacycle intermediate bonds to Ag(110) through both ends of the molecule, binding of EpB is strengthened relative to simple epoxides, stabilizing the oxametallacycle to relatively high temperatures (500 K). These studies of the interaction of EpB with Ag(110) have provided some insights as to how the bifunctional nature of the molecule influences its ability to react and bind with the surface, yet not much is known as to how EpB interacts with metals more associated with hydrogenation, including Pt.

In order to understand selectivity trends associated with the Ag–Pt/SiO$_2$ system, it is necessary to first understand how EpB interacts with the single-component surfaces. In this contribution, we study the interaction of EpB with the Pt(111) surface. Experiments were conducted after dosing EpB on Pt(111) using both high-resolution electron energy loss spectroscopy (HREELS) and temperature-programmed desorption (TPD) experiments. Density functional theory (DFT) calculations have also been employed to generate simple molecular models to aid the interpretation of experimental results. Comparison of the results presented here with other studies of EpB and crotonaldehyde,

a key EpB isomer, suggests possible mechanisms by which submonolayer Ag coverages may modify the selectivity of Pt catalysts.

2. Experimental and Theoretical Methods

All experiments were conducted in one of two ultrahigh vacuum chambers, kept at a base pressure of $<10^{-10}$ Torr. Both chambers have been described previously.[14] The first chamber was equipped with an LK3000 high-resolution electron energy loss spectrometer, manufactured by LK Technologies, and a sputter gun (Varian Model 981-2046) for sample cleaning via bombardment with Ar$^+$ ions. All HREELS experiments were performed in the specular direction. Spectra collected from these experiments were at a beam energy of 6.32 eV and had a full-width at half-maximum (fwhm) resolution of 3.9–4.6 meV for the elastically scattered beam. The second chamber was equipped with a quadrupole mass spectrometer from VG Scienta, a sputter gun for cleaning (LK Technologies Model NGI3000-SE), and equipment for LEED and AES experiments (LK Technologies Model RVL2000). Mass spectrometer fragmentation patterns for all products were determined by backfilling the chamber with each molecule. Except where noted otherwise, EpB was adsorbed onto the crystal surface using a direct dosing line that was lined up with the face of the Pt sample. Direct dosing was done to minimize contamination of the vacuum systems by EpB, which was found to be especially important in TPD experiments where background desorption after backdosing could be substantial. Because such exposures cannot be reported in Langmuirs, they are reported below in terms of TPD desorption yield. Additionally, all experiments that were conducted below room temperature were done using liquid nitrogen fed into a reservoir in thermal contact with the sample mount.

In all TPD experiments reported, the Pt sample was first cooled using liquid nitrogen to the reported temperatures. EpB was adsorbed on the surface using direct dosing through a tube aimed at the sample surface. The sample was then allowed to cool to below 123 K and was heated at a constant ramping rate of 2.2 K s^{-1}, while the mass spectrometer monitored mass/charge ratios ranging from 2 to 72. The main species detected by the mass spectrometer were EpB (tracked using $m/z = 70$), propylene ($m/z = 41$), CO ($m/z = 28$), and H$_2$ ($m/z = 2$). CO and H$_2$ coverages were determined by first calculating the standard peak area for saturation coverage of CO and H$_2$ on Pt(111) and then comparing the peak areas to those of the standard peaks.

The polished Pt(111) crystal was obtained from Princeton Scientific and cleaned using repeated cycles of Ar$^+$ ion sputtering (1–3 keV) and annealing at 1000–1100 K as well as heating in O$_2$ at approximately 773 K. Surface cleanliness was verified using O$_2$ TPD or HREELS. In both chambers, a 1.5 mm thick tantalum disk backing was used. The Pt sample was fit into a recess in the backing plate and held in place using two tantalum foil strips. The sample was heated using resistive heating by passing a current through tungsten wires. Both EpB at 98% purity and *trans*-crotonaldehyde at 98% purity were purchased from Sigma-Aldrich and were purified by using repeated freeze–pump–thaw cycles. Ultrahigh purity H$_2$ and O$_2$ were both purchased from Matheson Trigas; CO was purchased from Airgas.

The Amsterdam Density Functional (ADF) program was used for all DFT calculations.[15] Kohn–Sham one-electron equations were solved using the Vosko–Wilk–Nusair (VWN) functional.[16] ADF basis sets of double-ζ plus polarization (DZP) quality were employed for total energy calculations, whereas the basis set was extended to triple-ζ plus polarization (TZP) for frequency calcula-

(7) Schaal, M. T.; Williams, C. T.; Monnier, J. R. *J. Catal.* **2008**, in press.
(8) Schaal, M. T.; Metcalf, A. Y.; Montoya, J. H.; Wilkinson, J. P.; Stork, C. C.; Williams, C. T.; Monnier, J. R. *Catal. Today* **2007**, *123*, 142–150.
(9) Medlin, J. W.; Barteau, M. A.; Vohs, J. M. *J. Mol. Catal. A: Chem.* **2000**, *163*, 129–145.
(10) (a) Medlin, J. W.; Mavrikakis, M.; Barteau, M. A. *J. Phys. Chem. B* **1999**, *103*, 11169–11175. (b) Medlin, J. W.; Barteau, M. A. *J. Phys. Chem. B* **2001**, *105*, 10054–10061. (c) Medlin, J. W.; Sherrill, A. B.; Chen, J. G. G.; Barteau, M. A. *J. Phys. Chem. B* **2001**, *105*, 3769–3775.
(11) Campbell, C. T.; Paffett, M. T. *Surf. Sci.* **1986**, *177*, 417–430.
(12) Linic, S.; Barteau, M. A. *J. Am. Chem. Soc.* **2002**, *124*, 310–317.
(13) Lukaski, A. C.; Enever, M. C. N.; Barteau, M. A. *Surf. Sci.* **2007**, *601*, 3372–3382.

(14) Kershner, D. C.; Medlin, J. W. *Surf. Sci.* **2008**, *602*, 693–701.
(15) te Velde, G.; Bickelhaupt, F. M.; Baerends, E. J.; Fonseca Guerra, C.; van Gisbergen, S. J. A.; Snijders, J. G.; Ziegler, T. *J. Comput. Chem.* **2001**, *22*, 931–967.
(16) Vosko, S. H.; Wilk, L.; Nusair, M. *Can. J. Phys.* **1980**, *58*, 1200.
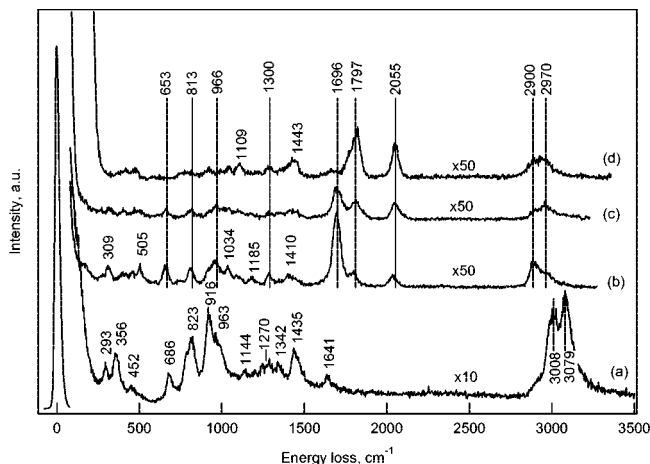
Figure 1. HREEL spectra of EpB adsorbed on Pt(111): (a) EpB condensed on Pt(111) at 91 K in a large direct dose; (b) EpB adsorbed after a saturating exposure at 233 K; (c) the surface in (b) annealed to 343 K; (d) the surface in (b) annealed to 403 K.

tions (see Supporting Information). All calculations were spin-unrestricted and employed the Becke[17] and Perdew[18] gradient approximations for the exchange and correlation energy terms, respectively. Atoms in the Pt cluster were held fixed at their experimental Pt−Pt distances for 10 and 15 atom Pt clusters, whereas all adsorbate atoms were allowed to fully relax. For calculations using Pt_3 clusters, all atoms were allowed to relax. To obtain theoretical vibrational spectra, two-point frequency calculations were performed on optimized adsorbate structures.

3. Results

In the presentation of results, we first address findings from HREELS to focus on the key surface transformations before considering TPD and DFT results, which provide additional insights into the relevant surface chemistry.

3.1. High-Resolution Electron Energy Loss Spectroscopy. A series of HREELS experiments was performed to track the thermal surface chemistry of EpB on Pt(111). The spectrum in Figure 1a depicts the HREEL spectrum after a large exposure of EpB onto Pt(111) at 91 K. As discussed below, this dose is sufficiently large that multilayers of EpB were condensed on the surface. The spectrum is in excellent agreement with that of EpB condensed on Ag(110) (Table 1). A few of the stronger features in the vibrational spectrum are the C−H and C−H$_2$ stretching peaks at 3079 and 3008 cm^{-1} as well as peaks at 916 cm^{-1} for C−H$_2$ twisting/rocking and at 823 cm^{-1} for symmetric deformations in O−C−C bonds.[9]

To determine how the adsorbed structure of EpB changes with increasing coverage, EpB was also adsorbed at increasingly higher exposures by backfilling the vacuum system. Figure 2 summarizes the results of these experiments. While overall consistency of the HREEL spectra suggests that EpB remains in its molecular state at both submonolayer (1 L) and multilayer (6 L) coverages, differences in the relative intensities of certain loss peaks provide insights into the structure of adsorbed EpB at low temperature. In particular, the C=C stretching peak at 1644 cm^{-1} observed after a 6 L exposure is absent in the spectra measured after subsaturation exposures. This result suggests that the C=C bond either is oriented parallel to the surface or has undergone rehybridization at submonolayer coverages, indicating
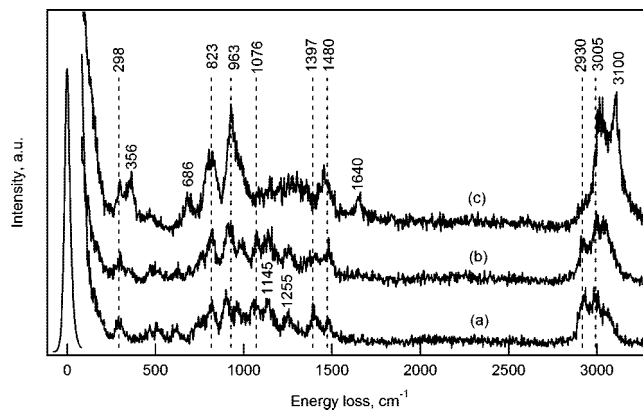
(17) Becke, A. D. *Phys. Rev. A* **1988**, *38*, 3098.
(18) Perdew, J. P. *Phys. Rev. B* **1986**, *33*, 8822.

Figure 2. HREEL spectra of EpB dosed at 105 K at various exposures: (a) 1.0 L; (b) 2.0 L; (c) 6.0 L.

Table 1. Vibrational Assignments for the HREELS Spectrum of EpB on Pt(111) at 91 K (Vibrational Frequencies in cm^{-1})

mode	liquid EpB[a]	EpB on Ag(110) at 140 K[a]	EpB on Pt(111) at 91 K
$\nu(C^2-H)/(C^3-H)$	2995	3051	3079
$\nu(C^1-H)/(C^4-H)$	2918	2951	3008
$\nu(C^3-C_4)$	1644	1654	1641
$X(C^4-H_2)$	1440	1433/1452	1435
$X(C^4H_2)$	1343	1347	1342
$\nu(C^1-C^2)$	1243	1243	1270
$\rho(C^1-H_2)$	1131	1138	1144
$B(C^3H)$	988	996	963
$\tau\omega(C^1-H_2)/\rho(C^4-H_2)$	915	917	916
$\delta_s(O-C^1-Cs)$	815	806	823
$\tau\omega(C^4-H_2)$	676	683	686
$\tau(C^2-C^3)$		363	356

^{a} Data taken from ref 9.

that the primary interaction of molecular EpB with the surface is through the olefin function. The lower-exposure spectrum also shows a large feature associated with C−H$_2$ stretching at ca. 2930 cm^{-1} that is relatively weaker in the multilayer spectrum. The significant decrease in this frequency relative to that associated with EpB multilayers is consistent with the olefin function rehybridizing into a di-σ sp^3-hybridized state on the surface, which is also the preferred state for ethylene on Pt(111) at similar temperatures.[19] It is also of interest to note the prominence of a small peak near 1076 cm^{-1} in the spectra associated with lower exposures, which is similar to the C−C stretching mode at 1040–1060 cm^{-1} observed in di-σ-bound ethylene.[20] Note that modes associated with the epoxide ring, particularly, the O−C−C deformation mode at 823 cm^{-1}, appear to be similar in the multilayer and epoxide states, indicating weak interaction of the epoxide with the surface. Many of the lower-frequency modes also shift slightly as EpB coverage is changed.

The thermal chemistry of EpB on Pt(111) was also investigated with HREELS. One of two experimental protocols was used. In the first, EpB was adsorbed onto the surface of Pt at a constant temperature of 233 K. After the exposure, the sample was allowed to cool to <110 K and the resultant HREEL spectrum was taken, as shown in Figure 1b. In the second, EpB

(19) Cremer, P. S.; Su, X. C.; Shen, Y. R.; Somorjai, G. A. *J. Am. Chem. Soc.* **1996**, *118*, 2942–2949.
(20) (a) Essen, J. M.; Haubrich, J.; Becker, C.; Wandelt, K. *Surf. Sci.* **2007**, *601*, 3472–3480. (b) Steininger, H.; Ibach, H.; Lehwald, S. *Surf. Sci.* **1982**, *117*, 685–698.
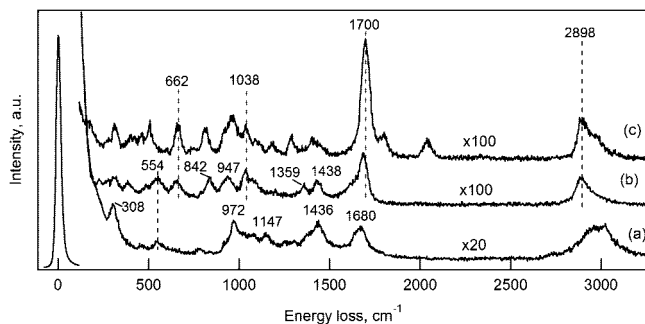
Figure 3. HREEL spectra of EpB and crotonaldehyde on Pt(111): (a) crotonaldehyde condensed on Pt(111) at 150 K; (b) crotonaldehyde condensed at 150 K and annealed to 233 K; (c) EpB dosed at 233 K.

Figure 4. Survey TPD of EpB on Pt(111).

was adsorbed at <110 K and annealed to 233 K before cooling and collecting the HREEL spectrum; these spectra were virtually indistinguishable from that shown in Figure 1b and are, therefore, not shown here. The reason for the use of two different dosing methods is related to the TPD experiments and is described in the following section. The 233 K spectrum differs greatly from that associated with molecular EpB (Figure 2a). The most significant difference is the strong peak at 1696 cm^{-1}, which is indicative of an aldehyde C=O bond.[21] We propose that, by 233 K, the EpB ring opens to form an aldehyde-like intermediate; assignments of the peaks for the intermediate and suggestions for its detailed structure are discussed below. Other experiments (not shown) indicate that the onset of the aldehyde formation reaction (where the 1696 cm^{-1} mode first appears) is between 180 and 200 K, and that the intermediate is detected even after relatively small exposures (1.0 L) of EpB at low temperature and subsequent annealing.

HREEL spectra of the surface after further annealing of the ring-opened EpB state derived at 233 K are shown in Figure 1c,d. As the temperature is increased, note the attenuation of the peak at 1696 cm^{-1} and the increase in intensity of peaks at 1797 and 2045 cm^{-1}. The peaks at 1797 and 2045 cm^{-1} are assigned to the C−O stretching mode of CO adsorbed on Pt(111) bridge sites and on top sites, respectively.[22] From this trend, it is clear that the proposed aldehyde intermediate on the surface undergoes decarbonylation starting before 233 K and nearly complete by 403 K. At temperatures above 450 K, CO desorbs from the surface.[21] In addition to CO, surface hydrocarbons are also formed as products from the decarbonylation.

As stated earlier, the aldehyde intermediate produced by 233 K has a strong peak at 1696 cm^{-1} that corresponds to the C=O bond of an aldehyde. Since crotonaldehyde (2-butenal) is an isomer of EpB, it is instructive to compare the thermal chemistry of *trans*-crotonaldehyde on Pt(111), which was previously studied by de Jesus and Zaera using reflection–absorption infrared spectroscopy (RAIRS)[21] and Haubrich et al.[23] using HREELS. Figure 3 shows a comparison of a spectrum measured following a 3.0 L dose of *trans*-crotonaldehyde at 150 K followed by annealing to 233 K with the spectrum measured for the EpB-derived intermediate at 233 K. While the two spectra are similar—both exhibit a strong C=O stretching loss at 1696 cm^{-1}, as well as a C−H aldehyde stretch at 2900 cm^{-1}—it is important to note that there are significant differ-
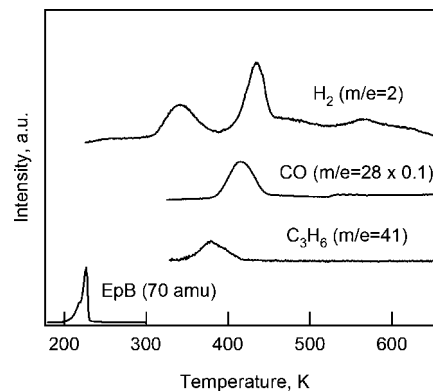
ences in the other loss features. Implications for differences between the sprectra are discussed below. The thermal chemistry of crotonaldehyde was also investigated by annealing to higher temperatures (not shown). As with the EpB intermediate, crotonaldehyde also undergoes decarbonylation, which is consistent with the findings of de Jesus et al.[21]

In studies of crotonaldehyde thermal chemistry on Pt(111), de Jesus noted that with crotonaldehyde the C=O peak is highly intense and is much more prominent than that for other aldehydes adsorbed on transition metal surfaces.[21,23-26] The high intensity of the C=O stretching loss is also apparent in Figure 3. The strong C=O peak in the spectrum likely indicates that the C=O bond in the intermediate is nearly perpendicular to the Pt surface. Furthermore, the peak position of 1696 cm^{-1} is indicative of a weak interaction between the aldehyde and the surface. Rather, it appears that binding of both crotonaldehyde and the EpB-derived aldehyde intermediate is dominated by the hydrocarbon end of the molecule. This point is further explored below.

3.2. Temperature-Programmed Desorption. TPD experiments were performed after adsorbing EpB at various exposures and temperatures. Figure 4 summarizes the desorption traces for all species detected in these experiments. Species desorbed were EpB in a peak near 230 K, propylene at 380 K, CO near 418 K, and H$_2$ in two peaks near 345 and 435 K. The desorption of C$_3$H$_6$, CO, and H$_2$ is consistent with a decarbonylation pathway that produces CO and C$_3$ hydrocarbon moieties on the surface.

Figure 5 shows the TPD traces of the decomposition products H$_2$, CO, and propylene as a function of total CO desorption yield for the various exposures used in this work. Assuming that all decomposition products are formed in a decarbonylation pathway, the CO coverage is equivalent to the coverage of the ring-opened aldehyde intermediate identified by HREELS at 233 K. These experiments were performed after exposures at 230 K, which assisted in deconvoluting the spectrum because of the absence of molecular EpB desorption from the background. Since EpB desorbs from Pt(111) near 230 K, contributions to the $m/e = 41$ signal from EpB could be avoided by exposures conducted at this temperature. The first trace in the series is that for H$_2$. At lower exposures (below CO desorption yields of 0.17 ML), H$_2$ has two main desorption peaks, the first at 340 K and the second at 430 K. Once the initial dose is increased

(21) de Jesus, J. C.; Zaera, F. *Surf. Sci.* **1999**, *430*, 99–115.
(22) Hopster, H.; Ibach, H. *Surf. Sci.* **1978**, *77*, 109–117.
(23) Haubrich, J.; Loffreda, D.; Delbecq, F.; Jugnet, Y.; Sautet, P.; Krupski, A.; Becker, C.; Wandelt, K. *Chem. Phys. Lett.* **2006**, *433*, 188–192.

(24) Brown, N. F.; Barteau, M. A. *J. Am. Chem. Soc.* **1992**, *114*, 4258–4265.
(25) Davis, J. L.; Barteau, M. A. *J. Am. Chem. Soc.* **1989**, *111*, 1782–1792.
(26) Houtman, C. J.; Barteau, M. A. *J. Catal.* **1991**, *130*, 528–546.
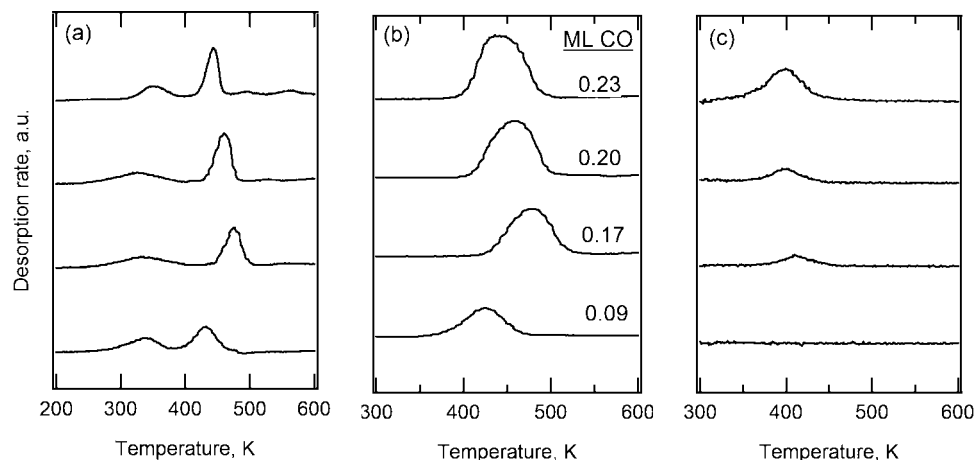
Figure 5. (a) H_2, (b) CO, and (c) propylene TPD traces for various EpB exposures; exposures are reported in total monolayers of CO desorbed.

so that the CO yield is 0.17 ML, the second peak shifts to 460 K, and both peaks change shape. There is also a difference in the relative peak areas for the low-temperature and high-temperature H_2 desorption states. At the lower exposures, the relative peak areas are approximately 50% in the first peak and 50% in the second peak. For the higher exposures, 30–38% of the area is in the first peak and 70–62% is in the second peak. This is in contrast to the findings of de Jesus et al. for crotonaldehyde, where, at a saturation exposure of 7.0 L, they found 50% of desorbed H_2 to be in the first peak and 50% to be in the second peak.[21]

The next trace in Figure 5 is for the desorption of CO at different EpB exposures. CO follows a similar trend as H_2, where the desorption peak undergoes a slight shift from 448 to 460 K at a CO yield of 0.17 ML. For increasing doses after 0.17 ML, the CO peak shifts to lower temperatures, down to about 424 K. The shift to lower desorption temperatures at higher exposures is a trend that has been seen in other work and is a result of repulsive interactions between neighboring CO molecules and/or adsorbed hydrocarbon moieties.[27]

The last series of traces is for propylene, which was tracked by monitoring the 41 amu signal. Propylene is not detected until higher EpB exposures are used, starting at CO yields of 0.17 ML. This indicates that C_3H_6 desorption only occurs at relatively high coverages, where interactions between adsorbates may disfavor complete decomposition of C_3 hydrocarbon intermediates. A balance around the CO and H_2 yield from C_4H_6O indicates that the maximum yield of propylene is <0.05 ML; that is, most adsorbates that proceed through decarbonylation undergo complete decomposition, even at saturation exposures.

Figure 6 shows a plot of desorption yield from each of the H_2 peaks and propylene as a function of total CO coverage. The low-temperature H_2 desorption yield at 340 K reaches a maximum coverage of ca. 0.20 ML at a total CO coverage of 0.17 ML; the second peak continues to increase up to 0.37 ML at the CO yield of 0.23 ML corresponding to saturation. Since the first peak represents the desorption-limited formation of H_2, it appears that higher coverages of the EpB-derived intermediate lead to suppression of low-temperature C–H activation. Furthermore, because the detection of propylene as a product coincides with the divergence of the high-temperature and low-temperature H_2 desorption yields, suppression of this low-
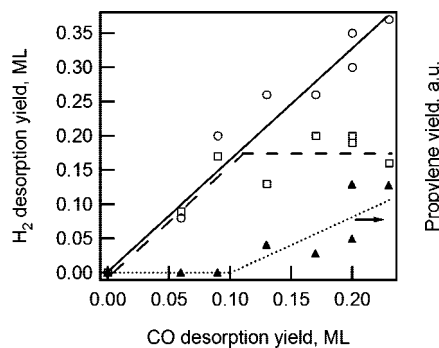
(27) Campbell, C. T.; Ertl, G.; Kuipers, H.; Segner, J. *Surf. Sci.* **1981**, *107*, 207–219.

Figure 6. H_2 (left-hand axis) and propylene (right-hand axis) desorption yields as a function of total CO yield, with lines included to guide the eye. Indicated on the plots is the absolute yield from the low-temperature H_2 desorption peak (open circles and dashed line) and high-temperature H_2 peak (open squares and solid line), as well as the relative propylene yield (closed triangles, dotted line).

temperature pathway may be related to the mechanism for propylene formation.

3.3. Density Functional Theory Calculations. DFT calculations were performed to address specific issues raised by the experimental results described above. The primary goal of these calculations was to aid in the identification of the aldehyde intermediate produced from EpB ring opening by 233 K. For comparisons to previous studies of EpB on Ag(110), the structure and stability of oxametallacycle intermediates (which were apparently not formed during experiments on Pt(111)) were also studied.

Initial efforts to identify the structure of the EpB-derived aldehyde intermediate focused on the assumption that the only molecular rearrangements of EpB were O–C^2 ring opening and C^1–H dissociation. Several starting geometries for this C_3H_4CHO intermediate were investigated (see Supporting Information). A strong interaction of the aldehyde function (in an η^4-bound state) was generally found to be thermodynamically favorable, contrary to observations from HREELS experiments indicated above. In an attempt to "artificially" break the interaction between the carbonyl function and the surface, clusters as small as Pt_3 were employed together with starting geometries in which the carbonyl was located at a remote position relative to the cluster. Even in these cases, however, the molecule was found to undergo reorientation to favor an
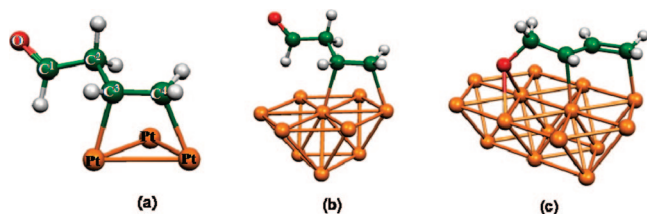
Figure 7. DFT-calculated equilibrium geometries on Pt clusters: (a) C_3H_6O aldehyde intermediate formed from H transfer from C^1 to C^2 on Pt_3 cluster; (b) intermediate from (a) on Pt_{10} cluster; (c) oxametallacycle intermediate on Pt_{15} cluster.
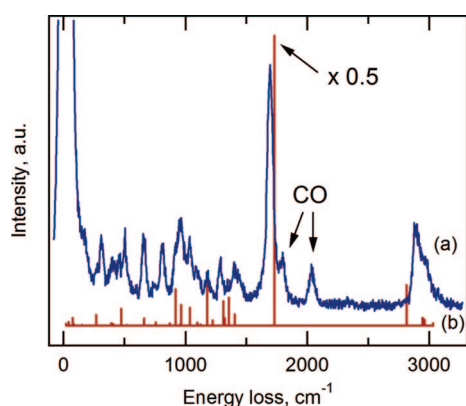

Figure 8. Comparison between experimental HREEL spectrum measured after adsorption of EpB at 233 K and DFT-computed IR spectrum for aldehyde intermediate depicted in Figure 7b.

η^4-like binding geometry and red-shifted (by >70 cm^{-1}) C=O stretching frequency, suggesting a strong driving force for such a process.

To explore alternative intermediates formed from EpB ring opening on Pt(111), a new assumption was made: that the dissociation of the C^1–H bond was accompanied by addition of H at the C^2 position to saturate that atom and create a C_3H_5CHO intermediate. The saturation of the C^2 atom helps to break the flat-lying coordination to the surface and results in an optimized structure on a Pt_3 cluster as shown in Figure 7a. As shown in Figure 8, the computed IR spectrum for this intermediate is in good agreement with the HREEL spectrum measured in Figure 1b, especially with respect to the intense C–O stretching vibration characteristic of an unbound aldehyde function. Agreement of the experimental and theoretical vibrational frequencies is also good when employing the $Pt_{10}(111)$ cluster (Figure 7c), as discussed below in detailed mode assignments. One important discrepancy, however, is that the Pt_{10} calculations indicated an agostic interaction between the Pt surface and the aldehyde H atom, as evidenced by a significantly red-shifted C^1–H stretching frequency of 2375 cm^{-1}; this interaction is not obvious from the experimental data and may be an artifact of cluster truncation effects or lack of surface crowding. The adsorption energy for the structure depicted in Figure 7c (at the DZP level) is –37 kcal/mol relative to free EpB, indicating favorable binding in this geometry.

Previous studies of the EpB chemistry on Ag(110) have shown that a multiply coordinated oxametallacycle is a highly stable intermediate. To test whether such intermediates should be favorable on Pt(111), geometry optimization of EpB-derived oxametallacycles has been performed on various Pt cluster sizes. Figure 7d shows a representative converged result. The binding

energy of –31 kcal/mol shows that the EpB-derived oxametallacycle is indeed stable (though somewhat less so than the aldehyde species described above), with a similar affinity as for Ag(110).[9] The oxametallacycle has C^2, C^3, and C^4 atoms in closer proximity to the surface on Pt(111) than on Ag(110), indicating (as expected) a stronger interaction with the hydrocarbon end of the molecule on Pt(111). Nevertheless, oxametallacycle intermediates are not observed in the experiments described above, likely due to a low barrier for C^1–H scission on the Pt surface, as discussed in more detail below.

4. Discussion

The discussion below considers three issues of primary importance. First, comparisons between the structure of the EpB-derived aldehyde intermediate and adsorbed crotonaldehyde are discussed. The adsorption and reaction of 1-epoxy-3-butene is then compared to the adsorption and reaction of other epoxides and unsaturated aldehydes on various single crystal surfaces. Last, we suggest how our findings relate to trends seen on bimetallic catalysts.

As indicated earlier, EpB ring opens on Pt(111) before 233 K to form an aldehyde intermediate. HREEL spectra for crotonaldehyde and EpB show similar loss features at 1696 and 2900 cm^{-1} (Figure 3). However, there are also numerous differences in the spectra. For example, the ring-opened EpB intermediate has a vibrational mode at 1440 cm^{-1} assigned to a C–H$_2$ scissoring motion, while this mode is absent from the crotonaldehyde spectrum.[9] Also, though both have loss peaks at around 2900 cm^{-1}, the EpB-derived intermediate also has a prominent shoulder at 2970 cm^{-1} consistent with C^4–H$_2$ stretching while crotonaldehyde does not.[9] Conversely, crotonaldehyde on Pt(111) has modes at 1340 and 1360 cm^{-1} that correspond to CH$_3$ deformations; these modes are not observed with the EpB intermediate.[21] Table 2 explains the proposed vibrational mode assignments in detail. The assignments were made through comparisons to DFT-computed vibrational spectra and with the known vibrational spectra of crotonaldehyde on Pt(111)[21,28] and EpB on Ag(110).[9]

In addition to the vibrational spectra, it is important to point out other similarities in the thermal chemistry of EpB and crotonaldehyde on Pt(111). Both the EpB-derived intermediate and crotonaldehyde undergo decarbonylation to produce CO, H$_2$, and propylene.[21] Subtle differences are present between the two chemistries, however. For example, EpB produces propylene in a peak at 380 K rather than the 340 K temperature found for crotonaldehyde. The somewhat higher temperature may result from the fact that production of propylene from EpB requires a hydrogenation step at two carbon atoms (C^2 and C^4), whereas only hydrogenation at the C^2 position is needed to produce propylene after decarbonylation of crotonaldehyde. It was also observed that the fraction of hydrogen desorbing in the high-temperature peak from EpB decomposition is higher than for crotonaldehyde decomposition, suggesting less complete decomposition of the EpB-derived intermediate at lower temperatures.

The adsorption and reaction of EpB on Pt(111) can also be compared to the reactions of other epoxides on single crystal surfaces. Medlin et al. studied EpB on Ag(110) at both low and moderate temperatures.[9] At low temperatures (140 K), they found that EpB molecularly adsorbs onto the surface and desorbs

(28) Oelichmann, H. J.; Bougeard, D.; Schrader, B. *J. Mol. Struct.* **1981**, *77*, 179–194.

Table 2. Vibrational Assigments for HREELS Spectrum of EpB-Derived Intermediate on Pt(111) at 233 K

mode	EpB on Pt(111) at 233 K	DFT calcd C_3H_6O/Pt_3	DFT calcd $C_3H_6O/Pt_{10}(111)$	EpB on Ag(110) at 140 K[a]	crotonaldehyde on Pt(111)[b]
$\nu(C^4-H)$	2970	2944–2964	2966/2953	2951	
$\nu(C^1-H)_{aldehyde}$	2900	2815	2375		2805
surface $\nu(C=O)$	2055				2055
surface $\nu(C=O)$	1797				1830
aldehyde $\nu(C=O)$	1696	1730	1731		1696
$\chi(C^4-H_2)$	1410	1404	1416	1433	
$\chi(C^2-H_2)$		1356	1370		
$b(C-H)$	1300	1322/1311	1313/1297		1300
$\tau\omega(C-H_2)$	1185	1178	1174		
$\nu(C-C)$	1092	1098	1089		1158
$\nu(C^1-C^2)$	1034	1038	1021		1083
$\rho(C^4-H_2)$	966	965	897		
$b(C^3-H)$, $\rho(C^4-H_2)$	933	918	937		
$\tau\omega(C-H_2)$	813	755	774	806	
$\tau\omega(C-H_2)$	653	661	618	683	
$\delta(O-C-C)$	505	519	492		
$\delta(C=C-C)$	463	472	428		464
$\nu(Pt-C)$	425	407			
$\nu(Pt-C)$	309				

[a] Data taken from ref 9. [b] Data taken from refs 21 and 28.

without reaction. At dosing temperatures close to 300 K, however, they found that EpB ring opens to form an oxametallacycle intermediate on the surface. Upon heating, the intermediate ring closed to form EpB as well as 2,5-dihydrofuran.[9]

The formation of an aldehyde from EpB must occur through scission of the C^2-O bond and, therefore, is likely mediated by a kinetically unstable oxametallacycle intermediate. As discussed above, formation of such an oxametallacycle has been found to be favorable on Pt(111) in DFT calculations. However, on Pt(111), ring opening is apparently accompanied by the essentially irreversible scission of a C^1-H bond. This points to an interesting facet of EpB chemistry on transition metal surfaces: while ring opening itself does not preclude retention of the epoxide ring in gas-phase products, C^1-H scission to produce the thermodynamically favored aldehyde—which occurs on more reactive surfaces such as Pt—does preclude reformation of the ring. This fact has important implications for catalysis of EpB, as discussed below.

The decomposition of the ring at higher temperatures is in accordance with trends seen with epoxides on other group VIII metals. Ethylene oxide (EtO) and/or propylene oxide decomposition has been studied on numerous surfaces. Studies of ethylene oxide on Cu(110) showed EtO to adsorb molecularly on the surface via the oxygen atom.[29] Similarly, Paffett and Campbell found that ethylene oxide adsorbs molecularly on Ag(110) at low temperatures and desorbs without reaction.[11] Other experiments performed on Ag(111) surfaces determined that EtO ring opened to form an oxametallacycle intermediate after higher-temperature exposures.[12] Paffett and Campbell also studied EtO on Pt(111) and found that EtO decomposes into CO and H_2 after adsorption at 110 K under conditions of low surface coverage of EtO.[11] This observation, however, was later disputed by Kim et al., who found that EtO does not undergo decomposition on Pt(111) at low temperatures; instead, it was found to adsorb reversibly on the Pt(111) surface.[30] EtO and propylene epoxide adsorption on Rh(111) has been studied by Brown and Barteau.[31] They found that both molecules adsorb

molecularly at low temperatures (91 K) and undergo decarbonylation around 230 K to yield CO and H_2; Brown and Barteau propose that the decomposition of the epoxides occurs via an oxametallacycle intermediate. On Pd(110), Shekhar et al. found ethylene oxide adsorbed molecularly onto the surface at 120 K.[32] At temperatures from 120 to 260 K, ethylene oxide ring opened through a proposed oxametallacycle intermediate to produce methylene and formyl/formaldehyde groups, which then decompose into CO and hydrogen. On Pd(111), however, EtO undergoes decomposition to yield ethylene and acetaldehyde,[33] which the authors postulate occurs through an oxametallacycle intermediate.

It is also worth reviewing experiments that have been performed with aldehydes on Rh(111), Pd(111), and Pt(111). Aldehydes on Pd(111) were found to form stable acyl intermediates in an η^2 configuration and decomposed via hydrogen removal from a methyl group and C—C bond scission to yield CO, hydrogen, and C_1 hydrocarbon fragments.[25] On the other hand, acetaldehyde decomposes on Rh(111) to produce CO, H_2, and CH_4 but forms in the $\eta^2(C,O)$ configuration and proceeds via methyl elimination.[26] Functional aldehydes such as acrolein and crotonaldehyde were also studied on Rh(111), Pd(111), and Pt(111). Brown and Barteau observed that acrolein adsorbed at low temperatures bound to Rh(111) with a $\eta^2(C,O)$ configuration, but annealing to 200 K caused its reconfiguration to an $\eta^4(C,C,C,O)$ form on the surface; decomposition yielded ethylene, ethane, CO, and H_2.[24] The authors suggest that acyl intermediates decompose via C—C scission, thereby releasing CO and an alkyl ligand one carbon shorter than the original aldehyde as its products. For acrolein, the C—C scission would yield a vinyl ligand on the surface.[24] On Pd(111), the authors found that acrolein also rehybridized to an $\eta^4(C,C,C,O)$ configuration and produced CO, H_2, ethylene, and propanal. In addition, they proposed that the oxygen atoms remain on the site of the main interaction with the surface, while the vinyl

(29) Benndorf, C.; Kruger, B.; Nieber, B. *Appl. Catal.* **1986**, *25*, 165–172.
(30) Kim, J.; Zhao, H. B.; Panja, C.; Olivas, A.; Koel, B. E. *Surf. Sci.* **2004**, *564*, 53–61.

(31) (a) Brown, N. F.; Barteau, M. A. *Surf. Sci.* **1993**, *298*, 6–17. (b) Brown, N. F.; Barteau, M. A. *J. Phys. Chem.* **1996**, *100*, 2269–2278.
(32) (a) Shekhar, R.; Barteau, M. A. *J. Vac. Sci. Technol. A* **1996**, *14*, 1469–1474. (b) Shekhar, R.; Barteau, M. A. *Surf. Sci.* **1996**, *348*, 55–66.
(33) Lambert, R. M.; Ormerod, R. M.; Tysoe, W. T. *Langmuir* **1994**, *10*, 730–733.

Scheme 1. Hydrogenation and Isomerization Pathways For EpB

Scheme 2. Decomposition Pathway for EpB on Pt(111)
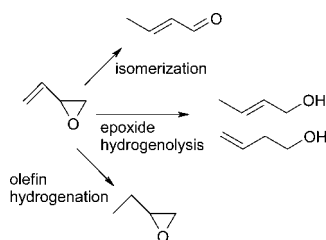
group modifies the coordination and reaction of the oxygenate.[34] Last, de Jesus et al. found that acrolein on Pt(111) decomposes to yield CO and ethylene,[35] by activation of the C−H bond followed by the loss of CO and rehydrogenation of the vinyl ligand. Decomposition also yields small amounts of ketene and propylene. [21]

The chemistry of EpB on Pt(111) has commonalities as well as differences with other epoxides on group VIII metals. At low temperatures, EpB adsorbs molecularly but decomposes above 200 K to release CO and H_2, as well as propylene. For epoxides adsorbed on Rh(111) and Pd(110), the authors propose that the adsorbed intermediate that undergoes decarbonylation is an oxametallacycle intermediate, decomposing via a reaction that is more similar to the corresponding alcohol rather than aldehyde.[31,32] In our experiments, however, it was found that that not only did the ring-opened intermediate have a structure somewhat similar to crotonaldehyde but it also underwent decomposition in a similar fashion as observed by TPD.[21]

One interesting result, as discussed above, is the apparently weak interaction of the aldehyde C=O function with the Pt(111) surface both for the EpB-derived intermediate and crotonaldehyde. In fact, the primary mode of interaction of molecular EpB and both the EpB- and crotonaldehyde-derived surface aldehyde intermediates does not appear to be through the oxygenate function but is rather through the hydrocarbon end of the molecule. This weak interaction is in sharp contrast with adsorption of acrolein on group VIII surfaces, where strong rehybridization of the C=O peak (and a weak loss feature) is observed. The presence of a fourth carbon atom in the bifunctional molecule thus apparently results in a significant reorientation of the molecule. In the case of EpB, where the C^4 atom is involved in an olefin functionality that is expected to interact with the surface, it is perhaps not unexpected that the carbon number affects adsorbate orientation of the aldehyde produced from ring opening. In the case of crotonaldehyde, however, the role of the terminal methyl group in reorienting the adsorbate away from an η^4 adsorption orientation is more surprising, especially in light of the fact that the methyl vibrational modes are not appreciably affected relative to the multilayer state. Further study is needed to understand the role of the terminal carbon atom in affecting adsorbate orientation.

On the basis of the results presented above, we can gain more insight into the reaction pathway for EpB on transition metals. In their paper studying the hydrogenation of EpB over bimetallic catalysts, Schaal et al. proposed a reaction scheme for the possible pathways of EpB hydrogenation, a simplified version of which is shown in Scheme 1.[7] EpB has three main reaction pathways: isomerization to crotonaldehyde, hydrogenation to
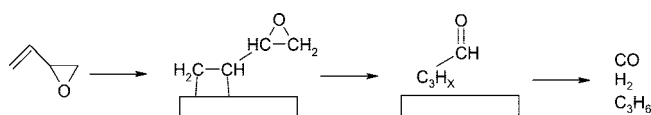
yield expxybutane, or hydrogenolysis to form 3-buten-1-ol and 2-buten-1-ol. Our experiments likely highlight the crotonaldehyde-mediated pathways, which have been observed to be dominant on supported Pt catalysts.[8] In our experiments, EpB is observed to decompose via the pathway shown in Scheme 2.

Since the thermal chemistry of EpB has now been investigated on both Pt(111) and Ag(110) surfaces, it is interesting to compare the results of these investigations with studies of bimetallic Ag−Pt catalysts. Schaal et al. conducted experiments to study the selectivity of the hydrogenation of EpB over a series of Ag−Pt/SiO_2 catalysts.[7] The bimetallic catalyst was prepared by loading different amounts of Ag onto a Pt/SiO_2 catalyst, and the selectivity to different products at each of the Ag weight loadings was monitored. The authors found that, as the nominal Ag coverage was increased from 0 to ca. ¼ ML, the selectivity of EpB to 1-epoxybutane increased dramatically. While EpB ring opens on both Ag(110) and Pt(111) surfaces, the ring-opened state can only undergo closure on Ag(110)—on Pt(111), ring opening is accompanied by irreversible C^1−H scission. It is therefore suggested that the role of Ag on the bimetallic catalyst is to interact with the epoxide end of the EpB molecule. Though ring opening to an oxametallacycle state likely still occurs, C^1−H scission leading to ring-opened gas-phase products is much less favorable. It is rather the regions of the catalyst surface consisting primarily of Pt that likely lead to aldehyde formation. However, the presence of Pt is essential for hydrogenation of the double-bond functionality. DFT calculations are currently being used to study EpB adsorption on various PtAg surfaces to test this hypothesis.

5. Conclusions

Adsorption and decomposition of EpB on Pt(111) has been studied using TPD, HREELS, and DFT calculations. EpB has been found to adsorb in a molecular state at low temperature, with an apparently stronger surface interaction with the double-bond function compared to the epoxide function. During thermal treatments, EpB decomposes by 230 K to produce a ring-opened aldehyde intermediate in which the aldehyde function interacts relatively weakly with the surface. Upon further heating, the intermediate undergoes decarbonylation to yield the gas-phase products CO, H_2, and propylene. The results presented here suggest that the improved olefin hydrogenation activity of Ag−Pt catalysts may be due to a bifunctional mechanism, whereby the oxygen-containing end of EpB interacts with Ag and the olefin function interacs with Pt.

Supporting Information Available: Further discussion of DFT modeling results and coordinates for all optimized geometries presented in Figure 7. This material is available free of charge via the Internet at http://pubs.acs.org.

(34) Davis, J. L.; Barteau, M. A. *J. Mol. Catal.* **1992**, *77*, 109–124.
(35) de Jesus, J. C.; Zaera, F. *J. Mol. Catal. A: Chem.* **1999**, *138*, 237–240.

JA711013N